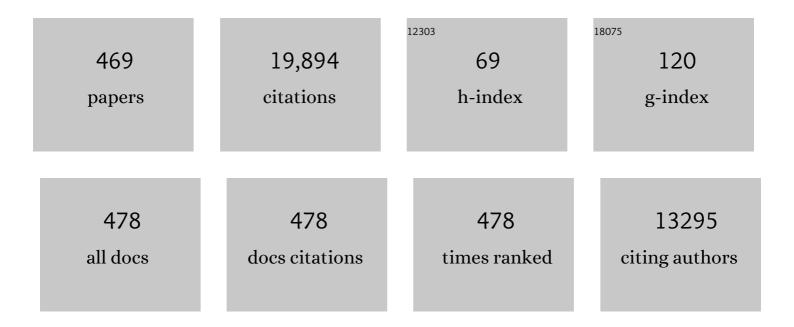
Mauritius C M Van De Sanden

List of Publications by Year in descending order

Source: https://exaly.com/author-pdf/4368415/publications.pdf Version: 2024-02-01



#	Article	IF	CITATIONS
1	The 2017 Plasma Roadmap: Low temperature plasma science and technology. Journal Physics D: Applied Physics, 2017, 50, 323001.	1.3	710
2	Plasma-Assisted Atomic Layer Deposition: Basics, Opportunities, and Challenges. Journal of Vacuum Science and Technology A: Vacuum, Surfaces and Films, 2011, 29, .	0.9	678
3	Ultralow surface recombination of c-Si substrates passivated by plasma-assisted atomic layer deposited Al2O3. Applied Physics Letters, 2006, 89, 042112.	1.5	646
4	On the c-Si surface passivation mechanism by the negative-charge-dielectric Al2O3. Journal of Applied Physics, 2008, 104, .	1.1	479
5	Silicon surface passivation by atomic layer deposited Al2O3. Journal of Applied Physics, 2008, 104, .	1.1	415
6	Surface passivation of highâ€efficiency silicon solar cells by atomicâ€layerâ€deposited Al ₂ O ₃ . Progress in Photovoltaics: Research and Applications, 2008, 16, 461-466.	4.4	414
7	Excellent passivation of highly doped p-type Si surfaces by the negative-charge-dielectric Al2O3. Applied Physics Letters, 2007, 91, .	1.5	370
8	Optical constants of graphene measured by spectroscopic ellipsometry. Applied Physics Letters, 2010, 97, .	1.5	348
9	Determining the material structure of microcrystalline silicon from Raman spectra. Journal of Applied Physics, 2003, 94, 3582-3588.	1.1	325
10	High efficiency n-type Si solar cells on Al2O3-passivated boron emitters. Applied Physics Letters, 2008, 92, .	1.5	316
11	<i>In situ</i> spectroscopic ellipsometry as a versatile tool for studying atomic layer deposition. Journal Physics D: Applied Physics, 2009, 42, 073001.	1.3	249
12	Vacancies and voids in hydrogenated amorphous silicon. Applied Physics Letters, 2003, 82, 1547-1549.	1.5	246
13	Plasma-assisted atomic layer deposition of Al2O3 moisture permeation barriers on polymers. Applied Physics Letters, 2006, 89, 081915.	1.5	244
14	Plasma and Thermal ALD of Al[sub 2]O[sub 3] in a Commercial 200â€,mm ALD Reactor. Journal of the Electrochemical Society, 2007, 154, G165.	1.3	237
15	Influence of the Deposition Temperature on the c-Si Surface Passivation by Al[sub 2]O[sub 3] Films Synthesized by ALD and PECVD. Electrochemical and Solid-State Letters, 2010, 13, H76.	2.2	198
16	Waveguide Nanowire Superconducting Single-Photon Detectors Fabricated on GaAs and the Study of Their Optical Properties. IEEE Journal of Selected Topics in Quantum Electronics, 2015, 21, 1-10.	1.9	188
17	Silicon surface passivation by ultrathin Al ₂ O ₃ films synthesized by thermal and plasma atomic layer deposition. Physica Status Solidi - Rapid Research Letters, 2010, 4, 10-12.	1.2	185
18	Hydrogen induced passivation of Si interfaces by Al2O3 films and SiO2/Al2O3 stacks. Applied Physics Letters, 2010, 97, .	1.5	168

#	Article	IF	CITATIONS
19	Conformality of Plasma-Assisted ALD: Physical Processes and Modeling. Journal of the Electrochemical Society, 2010, 157, G241.	1.3	157
20	Plasmaâ€driven dissociation of CO ₂ for fuel synthesis. Plasma Processes and Polymers, 2017, 14, 1600126.	1.6	152
21	Low Temperature Plasma-Enhanced Atomic Layer Deposition of Metal Oxide Thin Films. Journal of the Electrochemical Society, 2010, 157, P66.	1.3	151
22	Influence of the Oxidant on the Chemical and Field-Effect Passivation of Si by ALD Al[sub 2]O[sub 3]. Electrochemical and Solid-State Letters, 2011, 14, H1.	2.2	151
23	Controlling the fixed charge and passivation properties of Si(100)/Al2O3 interfaces using ultrathin SiO2 interlayers synthesized by atomic layer deposition. Journal of Applied Physics, 2011, 110, .	1.1	150
24	Taming microwave plasma to beat thermodynamics in CO ₂ dissociation. Faraday Discussions, 2015, 183, 233-248.	1.6	150
25	Stability of Al2O3 and Al2O3/a-SiNx:H stacks for surface passivation of crystalline silicon. Journal of Applied Physics, 2009, 106, .	1.1	145
26	<i>In Situ</i> Observation of Nanoparticle Exsolution from Perovskite Oxides: From Atomic Scale Mechanistic Insight to Nanostructure Tailoring. ACS Nano, 2019, 13, 12996-13005.	7.3	144
27	The 2022 Plasma Roadmap: low temperature plasma science and technology. Journal Physics D: Applied Physics, 2022, 55, 373001.	1.3	139
28	Thermodynamic generalization of the Saha equation for a two-temperature plasma. Physical Review A, 1989, 40, 5273-5276.	1.0	138
29	Influence of annealing and Al2O3 properties on the hydrogen-induced passivation of the Si/SiO2 interface. Journal of Applied Physics, 2012, 111, .	1.1	133
30	Negative charge and charging dynamics in Al2O3 films on Si characterized by second-harmonic generation. Journal of Applied Physics, 2008, 104,	1.1	131
31	display="inline"> <mml:mrow><mml:mi mathvariant="normal">Si<mml:mo>î—,</mml:mo><mml:mi mathvariant="normal">H</mml:mi </mml:mi </mml:mrow> stretching frequency to the nanostructural <mml:math <="" td="" xmlns:mml="http://www.w3.org/1998/Math/MathML"><td>1.1</td><td>123</td></mml:math>	1.1	123
32	Surface chemistry of plasma-assisted atomic layer deposition of Al2O3 studied by infrared spectroscopy. Applied Physics Letters, 2008, 92, .	1.5	117
33	Role of field-effect on c-Si surface passivation by ultrathin (2–20 nm) atomic layer deposited Al2O3. Applied Physics Letters, 2010, 96, .	1.5	117
34	A combined Thomson–Rayleigh scattering diagnostic using an intensified photodiode array. Review of Scientific Instruments, 1992, 63, 3369-3377.	0.6	113
35	Plasma chemistry aspects of a-Si:H deposition using an expanding thermal plasma. Journal of Applied Physics, 1998, 84, 2426-2435.	1.1	111
36	Surface reactions during atomic layer deposition of Pt derived from gas phase infrared spectroscopy. Applied Physics Letters, 2009, 95, .	1.5	111

#	Article	lF	CITATIONS
37	Atomic layer deposition for nanostructured Li-ion batteries. Journal of Vacuum Science and Technology A: Vacuum, Surfaces and Films, 2012, 30, .	0.9	111
38	Deposition of TiN and HfO2 in a commercial 200mm remote plasma atomic layer deposition reactor. Journal of Vacuum Science and Technology A: Vacuum, Surfaces and Films, 2007, 25, 1357-1366.	0.9	107
39	Remote Plasma ALD of Platinum and Platinum Oxide Films. Electrochemical and Solid-State Letters, 2009, 12, G34.	2.2	107
40	Oxygen Evolution at Hematite Surfaces: The Impact of Structure and Oxygen Vacancies on Lowering the Overpotential. Journal of Physical Chemistry C, 2016, 120, 18201-18208.	1.5	107
41	Evolution of the electrical and structural properties during the growth of Al doped ZnO films by remote plasma-enhanced metalorganic chemical vapor deposition. Journal of Applied Physics, 2007, 102, 043709.	1.1	106
42	Reaction mechanisms during plasma-assisted atomic layer deposition of metal oxides: A case study for Al2O3. Journal of Applied Physics, 2008, 103, .	1.1	101
43	Influence of the high-temperature "firing―step on high-rate plasma deposited silicon nitride films used as bulk passivating antireflection coatings on silicon solar cells. Journal of Vacuum Science & Technology an Official Journal of the American Vacuum Society B, Microelectronics Processing and Phenomena. 2003. 21. 2123.	1.6	99
44	In situ reaction mechanism studies of plasma-assisted atomic layer deposition of Al2O3. Applied Physics Letters, 2006, 89, 131505.	1.5	99
45	Hydrogenated amorphous silicon deposited at very high growth rates by an expanding Ar–H2–SiH4 plasma. Journal of Applied Physics, 2001, 89, 2404-2413.	1.1	98
46	Conformal Coverage of Poly(3,4-ethylenedioxythiophene) Films with Tunable Nanoporosity <i>via</i> Oxidative Chemical Vapor Deposition. ACS Nano, 2008, 2, 1959-1967.	7.3	97
47	In situspectroscopic ellipsometry study on the growth of ultrathin TiN films by plasma-assisted atomic layer deposition. Journal of Applied Physics, 2006, 100, 023534.	1.1	96
48	Efficient Plasma Route to Nanostructure Materials: Case Study on the Use of m-WO ₃ for Solar Water Splitting. ACS Applied Materials & Interfaces, 2013, 5, 7621-7625.	4.0	96
49	Substrate-biasing during plasma-assisted atomic layer deposition to tailor metal-oxide thin film growth. Journal of Vacuum Science and Technology A: Vacuum, Surfaces and Films, 2013, 31, .	0.9	95
50	CO and byproduct formation during CO2 reduction in dielectric barrier discharges. Journal of Applied Physics, 2014, 116, .	1.1	95
51	Low-Temperature Deposition of TiN by Plasma-Assisted Atomic Layer Deposition. Journal of the Electrochemical Society, 2006, 153, G956.	1.3	93
52	Argon-hydrogen plasma jet investigated by active and passive spectroscopic means. Physical Review E, 1994, 49, 4397-4406.	0.8	90
53	Homogeneous CO ₂ conversion by microwave plasma: Wave propagation and diagnostics. Plasma Processes and Polymers, 2017, 14, 1600120.	1.6	90
54	Surface textured ZnO films for thin film solar cell applications by expanding thermal plasma CVD. Thin Solid Films, 2001, 392, 226-230.	0.8	89

#	Article	IF	CITATIONS
55	Anomalous fast recombination in hydrogen plasmas involving rovibrational excitation. Physical Review E, 1993, 48, 2098-2102.	0.8	87
56	Deposition of TiN and TaN by Remote Plasma ALD for Cu and Li Diffusion Barrier Applications. Journal of the Electrochemical Society, 2008, 155, G287.	1.3	86
57	Recombination of argon in an expanding plasma jet. Physical Review E, 1993, 47, 2792-2797.	0.8	85
58	Optical and mechanical properties of plasmaâ€beamâ€deposited amorphous hydrogenated carbon. Journal of Applied Physics, 1996, 80, 5986-5995.	1.1	84
59	Formation of cationic silicon clusters in a remote silane plasma and their contribution to hydrogenated amorphous silicon film growth. Journal of Applied Physics, 1999, 86, 4029-4039.	1.1	78
60	The behaviour of heavy particles in the expanding plasma jet in argon. Plasma Sources Science and Technology, 1994, 3, 501-510.	1.3	77
61	Excellent Si surface passivation by low temperature SiO ₂ using an ultrathin Al ₂ O ₃ capping film. Physica Status Solidi - Rapid Research Letters, 2011, 5, 22-24.	1.2	77
62	Fluid modelling of CO2 dissociation in a dielectric barrier discharge. Journal of Applied Physics, 2016, 119, .	1.1	77
63	Synthesis andin situcharacterization of low-resistivity TaNx films by remote plasma atomic layer deposition. Journal of Applied Physics, 2007, 102, 083517.	1.1	75
64	<i>In situ</i> spectroscopic ellipsometry growth studies on the Al-doped ZnO films deposited by remote plasma-enhanced metalorganic chemical vapor deposition. Journal of Applied Physics, 2008, 103, .	1.1	73
65	Ion and Photon Surface Interaction during Remote Plasma ALD of Metal Oxides. Journal of the Electrochemical Society, 2011, 158, G88.	1.3	73
66	Surface passivation of phosphorusâ€diffused n ⁺ â€type emitters by plasmaâ€assisted atomicâ€layer deposited Al ₂ O ₃ . Physica Status Solidi - Rapid Research Letters, 2012, 6, 4-6.	1.2	73
67	Time evolution of vibrational temperatures in a CO ₂ glow discharge measured with infrared absorption spectroscopy. Plasma Sources Science and Technology, 2017, 26, 115008.	1.3	73
68	Highly efficient microcrystalline silicon solar cells deposited from a pure SiH4 flow. Applied Physics Letters, 2005, 87, 263503.	1.5	71
69	Plasma for electrification of chemical industry: a case study on CO ₂ reduction. Plasma Physics and Controlled Fusion, 2018, 60, 014019.	0.9	71
70	Absolute densities of N and excited N2 in a N2 plasma. Applied Physics Letters, 2003, 83, 4918-4920.	1.5	70
71	Local deposition of high-purity Pt nanostructures by combining electron beam induced deposition and atomic layer deposition. Journal of Applied Physics, 2010, 107, 116102.	1.1	70
72	The influence of partial surface discharging on the electrical characterization of DBDs. Plasma Sources Science and Technology, 2015, 24, 015016.	1.3	70

#	Article	IF	CITATIONS
73	The argon-hydrogen expanding plasma: model and experiments. Plasma Sources Science and Technology, 1995, 4, 74-85.	1.3	68
74	Amorphous silicon solar cells on natively textured ZnO grown by PECVD. Thin Solid Films, 2001, 392, 315-319.	0.8	68
75	Temperature dependence of the surface roughness evolution during hydrogenated amorphous silicon film growth. Applied Physics Letters, 2003, 82, 865-867.	1.5	68
76	High and intermediate temperature sodium–sulfur batteries for energy storage: development, challenges and perspectives. RSC Advances, 2019, 9, 5649-5673.	1.7	68
77	Effective passivation of Si surfaces by plasma deposited SiOx/a-SiNx:H stacks. Applied Physics Letters, 2011, 98, .	1.5	67
78	B-spline parametrization of the dielectric function applied to spectroscopic ellipsometry on amorphous carbon. Journal of Applied Physics, 2009, 106, .	1.1	66
79	Dielectric Properties of Thermal and Plasma-Assisted Atomic Layer Deposited Al[sub 2]O[sub 3] Thin Films. Journal of the Electrochemical Society, 2011, 158, G21.	1.3	65
80	Film growth precursors in a remote SiH[sub 4] plasma used for high-rate deposition of hydrogenated amorphous silicon. Journal of Vacuum Science and Technology A: Vacuum, Surfaces and Films, 2000, 18, 2153.	0.9	63
81	Detection of CH in an expanding argon/acetylene plasma using cavity ring down absorption spectroscopy. Chemical Physics Letters, 1999, 310, 405-410.	1.2	61
82	Cavity ring down study of the densities and kinetics of Si and SiH in a remote Ar-H2-SiH4 plasma. Journal of Applied Physics, 2001, 89, 2065-2073.	1.1	61
83	Effect of substrate conditions on the plasma beam deposition of amorphous hydrogenated carbon. Journal of Applied Physics, 1997, 82, 2643-2654.	1.1	59
84	On the formation mechanisms of the diffuse atmospheric pressure dielectric barrier discharge in CVD processes of thin silica-like films. Plasma Sources Science and Technology, 2009, 18, 045021.	1.3	59
85	Optical emission spectroscopy as a tool for studying, optimizing, and monitoring plasma-assisted atomic layer deposition processes. Journal of Vacuum Science and Technology A: Vacuum, Surfaces and Films, 2010, 28, 77-87.	0.9	59
86	Self-Regulated Plasma Heat Flux Mitigation Due to Liquid Sn Vapor Shielding. Physical Review Letters, 2016, 116, 135002.	2.9	59
87	Scaling of Si and GaAs trench etch rates with aspect ratio, feature width, and substrate temperature. Journal of Vacuum Science & Technology an Official Journal of the American Vacuum Society B, Microelectronics Processing and Phenomena, 1995, 13, 92.	1.6	58
88	An expanding thermal plasma for deposition of surface textured ZnO:Al with focus on thin film solar cell applications. Applied Surface Science, 2001, 173, 40-43.	3.1	58
89	Plasma beam deposited amorphous hydrogenated carbon: Improved film quality at higher growth rate. Applied Physics Letters, 1996, 69, 152-154.	1.5	57
90	High current diffuse dielectric barrier discharge in atmospheric pressure air for the deposition of thin silica-like films. Applied Physics Letters, 2010, 96, .	1.5	57

#	Article	IF	CITATIONS
91	Direct characterization of nanocrystal size distribution using Raman spectroscopy. Journal of Applied Physics, 2013, 114, 134310.	1.1	57
92	Molecular dynamics simulations for the growth of diamond-like carbon films from low kinetic energy species. Diamond and Related Materials, 2004, 13, 1873-1881.	1.8	56
93	Measurement of absolute radical densities in a plasma using modulated-beam line-of-sight threshold ionization mass spectrometry. Journal of Vacuum Science and Technology A: Vacuum, Surfaces and Films, 2004, 22, 71-81.	0.9	55
94	The importance of thermal dissociation in CO ₂ microwave discharges investigated by power pulsing and rotational Raman scattering. Plasma Sources Science and Technology, 2019, 28, 055015.	1.3	55
95	Composition and bonding structure of plasmaâ€assisted ALD Al ₂ O ₃ films. Physica Status Solidi C: Current Topics in Solid State Physics, 2010, 7, 976-979.	0.8	53
96	Towards Rollâ€ŧoâ€Roll Deposition of High Quality Moisture Barrier Films on Polymers by Atmospheric Pressure Plasma Assisted Process. Plasma Processes and Polymers, 2015, 12, 545-554.	1.6	53
97	Co-electrolysis of H2O and CO2 on exsolved Ni nanoparticles for efficient syngas generation at controllable H2/CO ratios. Applied Catalysis B: Environmental, 2019, 258, 117950.	10.8	53
98	Diagnostics of the magnetized lowâ€pressure hydrogen plasma jet: Molecular regime. Journal of Applied Physics, 1996, 80, 1312-1324.	1.1	52
99	Symmetrical Exsolution of Rh Nanoparticles in Solid Oxide Cells for Efficient Syngas Production from Greenhouse Gases. ACS Catalysis, 2020, 10, 1278-1288.	5.5	52
100	Plasma chemistry during the deposition of a-C:H films and its influence on film properties. Diamond and Related Materials, 2003, 12, 90-97.	1.8	51
101	Smooth and Self‧imilar SiO ₂ â€like Films on Polymers Synthesized in Rollâ€toâ€Roll Atmospheric Pressureâ€PECVD for Gas Diffusion Barrier Applications. Plasma Processes and Polymers, 2010, 7, 635-639.	1.6	51
102	Atomic layer deposition of Ru from CpRu(CO)2Et using O2 gas and O2 plasma. Journal of Vacuum Science and Technology A: Vacuum, Surfaces and Films, 2011, 29, .	0.9	51
103	Cross section for the mutual neutralization reactionH2++Hâ^', calculated in a multiple-crossing Landau-Zener approximation. Physical Review A, 1995, 51, 3362-3365.	1.0	50
104	Surface hydride composition of plasma deposited hydrogenated amorphous silicon: in situ infrared study of ion flux and temperature dependence. Surface Science, 2003, 530, 1-16.	0.8	50
105	Quasi-Ice Monolayer on Atomically Smooth AmorphousSiO2at Room Temperature Observed with a High-Finesse Optical Resonator. Physical Review Letters, 2005, 95, 166104.	2.9	50
106	Cavity ring down detection of SiH3 in a remote SiH4 plasma and comparison with model calculations and mass spectrometry. Journal of Vacuum Science and Technology A: Vacuum, Surfaces and Films, 2001, 19, 467-476.	0.9	49
107	Plasma-assisted atomic layer deposition of TiN/Al2O3 stacks for metal-oxide-semiconductor capacitor applications. Journal of Applied Physics, 2009, 106, .	1.1	49
108	Surface reaction probability during fast deposition of hydrogenated amorphous silicon with a remote silane plasma. Journal of Applied Physics, 2000, 87, 3313-3320.	1.1	47

#	Article	IF	CITATIONS
109	Abstraction of atomic hydrogen by atomic deuterium from an amorphous hydrogenated silicon surface. Journal of Chemical Physics, 2002, 117, 10805-10816.	1.2	47
110	Threshold ionization mass spectrometry of reactive species in remote Arâ^•C2H2 expanding thermal plasma. Journal of Vacuum Science and Technology A: Vacuum, Surfaces and Films, 2005, 23, 1400-1412.	0.9	46
111	Atmospheric Pressure Barrier Discharge Deposition of Silica-Like Films on Polymeric Substrates. Plasma Processes and Polymers, 2007, 4, S440-S444.	1.6	46
112	High Quality SiO ₂ â€like Layers by Large Area Atmospheric Pressure Plasma Enhanced CVD: Deposition Process Studies by Surface Analysis. Plasma Processes and Polymers, 2009, 6, 693-702.	1.6	46
113	Substrate Biasing during Plasma-Assisted ALD for Crystalline Phase-Control of TiO2 Thin Films. Electrochemical and Solid-State Letters, 2011, 15, G1-G3.	2.2	46
114	Characterization of plasma beam deposited amorphous hydrogenated silicon. Applied Physics Letters, 1995, 67, 491-493.	1.5	45
115	High-rate plasma-deposited SiO2 films for surface passivation of crystalline silicon. Journal of Vacuum Science and Technology A: Vacuum, Surfaces and Films, 2006, 24, 1823-1830.	0.9	45
116	Implications of thermo-chemical instability on the contracted modes in CO ₂ microwave plasmas. Plasma Sources Science and Technology, 2020, 29, 025005.	1.3	45
117	Plasma Activated Electrochemical Ammonia Synthesis from Nitrogen and Water. ACS Energy Letters, 2021, 6, 313-319.	8.8	44
118	Oscillatory vapour shielding of liquid metal walls in nuclear fusion devices. Nature Communications, 2017, 8, 192.	5.8	43
119	Hydrogen poor cationic silicon clusters in an expanding argon–hydrogen–silane plasma. Applied Physics Letters, 1998, 72, 2397-2399.	1.5	42
120	The heating mechanism of electrons in the shock front of an expanding plasma. Plasma Sources Science and Technology, 1994, 3, 511-520.	1.3	41
121	Time-resolved cavity ringdown study of the Si and SiH3 surface reaction probability during plasma deposition of a-Si:H at different substrate temperatures. Journal of Applied Physics, 2004, 96, 4094-4106.	1.1	41
122	Electrochemical Activation of Atomic Layer-Deposited Cobalt Phosphate Electrocatalysts for Water Oxidation. ACS Catalysis, 2021, 11, 2774-2785.	5.5	41
123	Industrial high-rate (â^145 nm/s) deposited silicon nitride yielding high-quality bulk and surface passivation under optimum anti-reflection coating conditions. Progress in Photovoltaics: Research Real-ti្នាម៉ីឲដប់dyស្នាឱថាភ្នាំ:អាងដល់ភាពនាmml="http://www.w3.org/1998/Math/MathML"	4.4	40
124	display="inline"> <mml:mrow><mml:mi>a</mml:mi><mml:mtext>â^'</mml:mtext>cmml:mi mathvariant="normal">Si<mml:mo>:</mml:mo><mml:mi mathvariant="normal">H<mml:mo>â^•</mml:mo><mml:mi>c</mml:mi><mml:mtext>â^'</mml:mtext> mathvariant="normal">Si</mml:mi </mml:mrow> heterointerface formation and epitaxial	<nnnl:mi</n	40
125	Si growth by spectroscopic ellipsometry, infrared spectroscopy, and second-harmonic generation. Bhy Surface Hydride Composition of Plasma-Synthesized Si Nanoparticles. Journal of Physical Chemistry C, 2011, 115, 20375-20379.	1.5	40
126	Nanostructuring of Iron Surfaces by Low-Energy Helium Ions. ACS Applied Materials & Interfaces, 2014, 6, 3462-3468.	4.0	40

#	Article	IF	CITATIONS
127	Quantum Magnetoconductance of a Nondegenerate Two-Dimensional Electron Gas. Europhysics Letters, 1988, 6, 75-80.	0.7	39
128	Production Mechanisms of NH and NH ₂ Radicals in N ₂ â^'H ₂ Plasmas. Journal of Physical Chemistry A, 2007, 111, 11460-11472.	1.1	39
129	The atomic hydrogen flux to silicon growth flux ratio during microcrystalline silicon solar cell deposition. Applied Physics Letters, 2008, 93, 111914.	1.5	39
130	Surface Modifications Induced by High Fluxes of Low Energy Helium Ions. Scientific Reports, 2015, 5, 9779.	1.6	39
131	High-rate deposition of a-SiNx:H for photovoltaic applications by the expanding thermal plasma. Journal of Vacuum Science and Technology A: Vacuum, Surfaces and Films, 2002, 20, 1704-1715.	0.9	38
132	Optical second-harmonic generation in thin film systems. Journal of Vacuum Science and Technology A: Vacuum, Surfaces and Films, 2008, 26, 1519-1537.	0.9	38
133	Effect of ion bombardment on the a-Si:H based surface passivation of c-Si surfaces. Applied Physics Letters, 2011, 98, .	1.5	38
134	Quality improvement of plasma-beam-deposited amorphous hydrogenated carbon with higher growth rate. Plasma Sources Science and Technology, 1996, 5, 492-498.	1.3	37
135	Argon ion-induced dissociation of acetylene in an expanding Ar/C2H2 plasma. Applied Physics Letters, 1999, 74, 2927-2929.	1.5	37
136	Direct and highly sensitive measurement of defect-related absorption in amorphous silicon thin films by cavity ringdown spectroscopy. Applied Physics Letters, 2004, 84, 3079-3081.	1.5	37
137	The effect of ion-surface and ion-bulk interactions during hydrogenated amorphous silicon deposition. Journal of Applied Physics, 2007, 102, 073523.	1.1	37
138	Real time in situ spectroscopic ellipsometry of the growth and plasmonic properties of au nanoparticles on SiO2. Nano Research, 2012, 5, 513-520.	5.8	37
139	Four ways to determine the electron density in low-temperature plasmas. Physical Review E, 1994, 49, 2272-2275.	0.8	36
140	Ultrahigh throughput plasma processing of free standing silicon nanocrystals with lognormal size distribution. Journal of Applied Physics, 2013, 113, .	1.1	36
141	CO ₂ Conversion in Nonuniform Discharges: Disentangling Dissociation and Recombination Mechanisms. Journal of Physical Chemistry C, 2020, 124, 16806-16819.	1.5	36
142	Stationary supersonic plasma expansion: continuum fluid mechanics versus direct simulation Monte Carlo method. Journal Physics D: Applied Physics, 2002, 35, 1362-1372.	1.3	35
143	Time-resolved cavity ring-down spectroscopic study of the gas phase and surface loss rates of Si and SiH3 plasma radicals. Chemical Physics Letters, 2002, 360, 189-193.	1.2	35
144	Plasma diagnostic study of silicon nitride film growth in a remote Ar–H2–N2–SiH4 plasma: Role of N and SiHn radicals. Journal of Vacuum Science and Technology A: Vacuum, Surfaces and Films, 2004, 22, 96-106.	0.9	35

#	Article	IF	CITATIONS
145	Atmospheric glow stabilization. Do we need pre-ionization?. Surface and Coatings Technology, 2005, 200, 46-50.	2.2	35
146	On the hexamethyldisiloxane dissociation paths in a remote Ar-fed expanding thermal plasma. Plasma Sources Science and Technology, 2006, 15, 421-431.	1.3	35
147	On the role of nanoporosity in controlling the performance of moisture permeation barrier layers. Microporous and Mesoporous Materials, 2014, 188, 163-171.	2.2	35
148	Insight into CO ₂ Dissociation in Plasma from Numerical Solution of a Vibrational Diffusion Equation. Journal of Physical Chemistry C, 2017, 121, 19568-19576.	1.5	35
149	Plasma-Activated Electrolysis for Cogeneration of Nitric Oxide and Hydrogen from Water and Nitrogen. ACS Energy Letters, 2019, 4, 2091-2095.	8.8	35
150	Emission spectroscopy on a supersonically expanding argon/silane plasma. Journal of Applied Physics, 1992, 71, 4156-4163.	1.1	34
151	Effect of hydrogen on the growth of thin hydrogenated amorphous carbon films from thermal energy radicals. Applied Physics Letters, 2006, 88, 141922.	1.5	34
152	Accurate control of ion bombardment in remote plasmas using pulse-shaped biasing. Journal of Applied Physics, 2009, 106, 073303.	1.1	34
153	Fast deposition of amorphous carbon films by an expanding cascaded arc plasma jet. Journal of Applied Physics, 1995, 78, 528-540.	1.1	33
154	Temperature dependence of the surface reactivity of SiH3 radicals and the surface silicon hydride composition during amorphous silicon growth. Surface Science, 2003, 547, L865-L870.	0.8	33
155	Analysis of the expanding thermal argon–oxygen plasma gas phase. Plasma Sources Science and Technology, 2003, 12, 539-553.	1.3	33
156	Improvement of hydrogenated amorphous silicon properties with increasing contribution of SiH3 to film growth. Journal of Vacuum Science and Technology A: Vacuum, Surfaces and Films, 2001, 19, 1027-1029.	0.9	32
157	Role of carbon atoms in the remote plasma deposition of hydrogenated amorphous carbon. Journal of Applied Physics, 2003, 94, 6932-6938.	1.1	32
158	Transient depletion of source gases during materials processing: a case study on the plasma deposition of microcrystalline silicon. New Journal of Physics, 2007, 9, 280-280.	1.2	32
159	Initiated-chemical vapor deposition of organosilicon layers: Monomer adsorption, bulk growth, and process window definition. Journal of Vacuum Science and Technology A: Vacuum, Surfaces and Films, 2012, 30, .	0.9	32
160	Amorphous hydrogenated carbon nitride films deposited via an expanding thermal plasma at high growth rates. Thin Solid Films, 1998, 333, 29-34.	0.8	31
161	In situprobing of surface hydrides on hydrogenated amorphous silicon using attenuated total reflection infrared spectroscopy. Journal of Vacuum Science and Technology A: Vacuum, Surfaces and Films, 2002, 20, 781-789.	0.9	31
162	Threshold ionization mass spectrometry study of hydrogenated amorphous carbon films growth precursors. Chemical Physics Letters, 2005, 402, 37-42.	1.2	31

#	Article	IF	CITATIONS
163	Plasma-assisted atomic layer deposition of TiN monitored byin situspectroscopic ellipsometry. Journal of Vacuum Science and Technology A: Vacuum, Surfaces and Films, 2005, 23, L5-L8.	0.9	31
164	Microcrystalline silicon deposition: Process stability and process control. Thin Solid Films, 2007, 515, 7455-7459.	0.8	31
165	Evidence of the filling of nano-porosity in SiO2-like layers by an initiated-CVD monomer. Microporous and Mesoporous Materials, 2012, 151, 434-439.	2.2	31
166	Depolarization Rayleigh scattering as a means of molecular concentration determination in plasmas. Physical Review Letters, 1992, 69, 1379-1382.	2.9	30
167	Spectroscopic measurement of atomic hydrogen level populations and hydrogen dissociation degree in expanding cascaded arc plasmas. Journal of Applied Physics, 1994, 76, 4499-4510.	1.1	30
168	Dissociative recombination in cascaded arc generated Ar–N2and N2expanding plasma. Physics of Plasmas, 1994, 1, 2086-2095.	0.7	30
169	Density and production of NH and NH2 in an Ar–NH3 expanding plasma jet. Journal of Applied Physics, 2005, 98, 093301.	1.1	30
170	Microcrystalline silicon solar cells with an open-circuit voltage above 600mV. Applied Physics Letters, 2007, 90, 183504.	1.5	30
171	Deposition of highly efficient microcrystalline silicon solar cells under conditions of low H2 dilution: the role of the transient depletion induced incubation layer. Progress in Photovoltaics: Research and Applications, 2007, 15, 291-301.	4.4	30
172	On the oxidation mechanism of microcrystalline silicon thin films studied by Fourier transform infrared spectroscopy. Journal of Non-Crystalline Solids, 2011, 357, 884-887.	1.5	30
173	Zeolites for CO ₂ –CO–O ₂ Separation to Obtain CO ₂ -Neutral Fuels. ACS Applied Materials & Interfaces, 2018, 10, 20512-20520.	4.0	30
174	Characterization of CO ₂ microwave plasma based on the phenomenon of skin-depth-limited contraction. Plasma Sources Science and Technology, 2019, 28, 115022.	1.3	30
175	Absorption spectroscopy on the argon first excited state in an expanding thermal arc plasma. Physical Review E, 1994, 50, 1383-1393.	0.8	29
176	Hard graphitelike hydrogenated amorphous carbon grown at high rates by a remote plasma. Journal of Applied Physics, 2010, 107, .	1.1	29
177	Wall Association and Recirculation in Expanding Thermal Arc Plasmas. Physical Review Letters, 1996, 76, 1840-1843.	2.9	28
178	Langmuir probe measurements in an expanding magnetized plasma. Physical Review E, 1996, 54, 1906-1911.	0.8	28
179	Deposition of a-Si:H and a-C:H using an expanding thermal arc plasma. Plasma Sources Science and Technology, 1996, 5, 268-274.	1.3	28
180	Characterization of carbon nitride thin films deposited by a combined RF and DC plasma beam. Thin Solid Films, 1998, 325, 123-129.	0.8	28

#	Article	IF	CITATIONS
181	Argon–oxygen plasma treatment of deposited organosilicon thin films. Thin Solid Films, 2004, 449, 40-51.	0.8	28
182	The Staebler-Wronski Effect: New Physical Approaches and Insights as a Route to Reveal its Origin. Materials Research Society Symposia Proceedings, 2010, 1245, 1.	0.1	28
183	Remote Plasma ALD of SrTiO[sub 3] Using Cyclopentadienlyl-Based Ti and Sr Precursors. Journal of the Electrochemical Society, 2011, 158, G34.	1.3	28
184	The Relation Between the Bandgap and the Anisotropic Nature of Hydrogenated Amorphous Silicon. IEEE Journal of Photovoltaics, 2012, 2, 94-98.	1.5	28
185	Mechanism and activation energy barrier for H abstraction by H(D) from a-Si:H surfaces. Surface Science, 2002, 515, L469-L474.	0.8	27
186	Stripping of photoresist using a remote thermal Ar/O[sub 2] and Ar/N[sub 2]/O[sub 2] plasma. Journal of Vacuum Science & Technology an Official Journal of the American Vacuum Society B, Microelectronics Processing and Phenomena, 2003, 21, 61.	1.6	27
187	Optical and chemical characterization of expanding thermal plasma deposited silicon dioxide-like films. Thin Solid Films, 2005, 484, 104-112.	0.8	27
188	Plasma-assisted atomic layer deposition of Ta2O5 from alkylamide precursor and remote O2 plasma. Journal of Vacuum Science and Technology A: Vacuum, Surfaces and Films, 2008, 26, 472-480.	0.9	27
189	Novel approach to thin film polycrystalline silicon on glass. Materials Letters, 2009, 63, 1817-1819.	1.3	27
190	<i>In situ</i> spectroscopic ellipsometry during atomic layer deposition of Pt, Ru and Pd. Journal Physics D: Applied Physics, 2016, 49, 115504.	1.3	27
191	Excitation and relaxation of the asymmetric stretch mode of CO ₂ in a pulsed glow discharge. Plasma Sources Science and Technology, 2019, 28, 035011.	1.3	27
192	Insight into contraction dynamics of microwave plasmas for CO ₂ conversion from plasma chemistry modelling. Plasma Sources Science and Technology, 2020, 29, 105014.	1.3	27
193	Cavity ring down detection of SiH3 on the broadband à 2A1′ ↕X̃ 2A1 transition in a remote Ar–H2–Si plasma. Chemical Physics Letters, 2000, 326, 400-406.	H4 1.2	25
194	Detailed TIMS Study of Ar/C2H2Expanding Thermal Plasma:Â Identification of a-C:H Film Growth Precursors. Journal of Physical Chemistry A, 2005, 109, 10153-10167.	1.1	25
195	Ammonia adsorption and decomposition on silica supported Rh nanoparticles observed by in situ attenuated total reflection infrared spectroscopy. Applied Surface Science, 2006, 253, 572-580.	3.1	25
196	Er3+ and Si luminescence of atomic layer deposited Er-doped Al2O3 thin films on Si(100). Journal of Applied Physics, 2011, 109, .	1.1	25
197	A rotational Raman study under non-thermal conditions in a pulsed CO ₂ glow discharge. Plasma Sources Science and Technology, 2018, 27, 045009.	1.3	25
198	Nonâ€oxidative methane coupling to C ₂ hydrocarbons in a microwave plasma reactor. Plasma Processes and Polymers, 2018, 15, 1800087.	1.6	25

#	Article	IF	CITATIONS
199	Hydrogen in a-Si:H Deposited by an Expanding Thermal Plasma: A Temperature, Growth Rate and Isotope Study. Materials Research Society Symposia Proceedings, 1998, 507, 529.	0.1	24
200	Plasma chemistry of an expanding Ar/C2H2 plasma used for fast deposition of a-C:H. Diamond and Related Materials, 1999, 8, 677-681.	1.8	24
201	Unraveling the deposition mechanism in a-C:H thin-film growth: A molecular-dynamics study for the reaction behavior of C3 and C3H radicals with a-C:H surfaces. Journal of Applied Physics, 2006, 99, 014902.	1.1	24
202	Note: Rotational Raman scattering on CO2 plasma using a volume Bragg grating as a notch filter. Review of Scientific Instruments, 2015, 86, 046106.	0.6	24
203	Use ofin situFTIR spectroscopy and mass spectrometry in an expanding hydrocarbon plasma. Plasma Sources Science and Technology, 2000, 9, 615-624.	1.3	23
204	Investigation of processes in low-pressure expanding thermal plasmas used for carbon nitride deposition: I. Ar/N2/C2H2plasma. Plasma Sources Science and Technology, 2001, 10, 513-523.	1.3	23
205	Bulk passivation of multicrystalline silicon solar cells induced by high-rate-deposited (> 1 nm/s) silicon nitride films. Progress in Photovoltaics: Research and Applications, 2003, 11, 125-130.	4.4	23
206	Expanding thermal plasma for low-k dielectrics: engineering the film chemistry by means of specific dissociation paths in the plasma. Materials Science in Semiconductor Processing, 2004, 7, 283-288.	1.9	23
207	Dry etching of surface textured zinc oxide using a remote argon–hydrogen plasma. Applied Surface Science, 2005, 241, 321-325.	3.1	23
208	Surface-diffusion-controlled incorporation of nanosized voids during hydrogenated amorphous silicon film growth. Applied Physics Letters, 2005, 86, 041909.	1.5	23
209	Optical properties of Y2O3 thin films doped with spatially controlled Er3+ by atomic layer deposition. Journal of Applied Physics, 2007, 101, .	1.1	23
210	Remote Plasma Deposited Silicon Dioxideâ€Like Film Densification by Means of RF Substrate Biasing: Film Chemistry and Morphology. Plasma Processes and Polymers, 2007, 4, 621-628.	1.6	23
211	An Electrochemical Study on the Cathode of the Intermediate Temperature Tubular Sodium-Sulfur (NaS) Battery. Journal of the Electrochemical Society, 2019, 166, A135-A142.	1.3	23
212	Observation and rationalization of nitrogen oxidation enabled only by coupled plasma and catalyst. Nature Communications, 2022, 13, 402.	5.8	23
213	Spectroscopic second harmonic generation measured on plasma-deposited hydrogenated amorphous silicon thin films. Applied Physics Letters, 2004, 85, 4049-4051.	1.5	22
214	N, NH, and NH2 radical densities in a remote Ar–NH3–SiH4 plasma and their role in silicon nitride deposition. Journal of Applied Physics, 2006, 100, 093303.	1.1	22
215	Reaction mechanisms of atomic layer deposition of TaNx from Ta(NMe2)5 precursor and H2-based plasmas. Journal of Vacuum Science and Technology A: Vacuum, Surfaces and Films, 2012, 30, 01A101.	0.9	22
216	On the intrinsic moisture permeation rate of remote microwave plasma-deposited silicon nitride layers. Thin Solid Films, 2014, 558, 54-61.	0.8	22

#	Article	IF	CITATIONS
217	Molecular dynamics simulations of ballistic He penetration into W fuzz. Nuclear Fusion, 2016, 56, 126015.	1.6	22
218	CO2-Neutral Fuels. Europhysics News, 2016, 47, 22-26.	0.1	22
219	Validation of the Fokker–Planck Approach to Vibrational Kinetics in CO ₂ Plasma. Journal of Physical Chemistry C, 2019, 123, 22823-22831.	1.5	22
220	Numerical model for the determination of the reduced electric field in a CO ₂ microwave plasma derived by the principle of impedance matching. Plasma Sources Science and Technology, 2019, 28, 075016.	1.3	22
221	Plasma activation of N ₂ , CH ₄ and CO ₂ : an assessment of the vibrational non-equilibrium time window. Plasma Sources Science and Technology, 2020, 29, 115001.	1.3	22
222	High-quality a–Si:H grown at high rate using an expanding thermal plasma. Surface and Coatings Technology, 1997, 97, 719-722.	2.2	21
223	Deposition of organosilicon thin films using a remote thermal plasma. Thin Solid Films, 2004, 449, 52-62.	0.8	21
224	Opportunities for Plasma-Assisted Atomic Layer Deposition. ECS Transactions, 2007, 3, 183-190.	0.3	21
225	The effect of low frequency pulse-shaped substrate bias on the remote plasma deposition of a-Si : H thin films. Plasma Sources Science and Technology, 2010, 19, 015012.	1.3	21
226	On the Effect of the Amorphous Silicon Microstructure on the Grain Size of Solid Phase Crystallized Polycrystalline Silicon. Advanced Energy Materials, 2011, 1, 401-406.	10.2	21
227	The relation between the production efficiency of nitrogen atoms and the electrical characteristics of a dielectric barrier discharge. Plasma Sources Science and Technology, 2015, 24, 045006.	1.3	21
228	Atmospheric pressure rollâ€toâ€roll plasma enhanced CVD of high quality silicaâ€like bilayer encapsulation films. Plasma Processes and Polymers, 2017, 14, 1600143.	1.6	21
229	Hydrogen atom cleaning of archeological artefacts. Journal of Nuclear Materials, 1993, 200, 380-382.	1.3	20
230	Formation of large positive silicon-cluster ions in a remote silane plasma. Journal of Vacuum Science and Technology A: Vacuum, Surfaces and Films, 1999, 17, 1531-1535.	0.9	20
231	Ellipsometric characterization of expanding thermal plasma deposited SiO2-like films. Thin Solid Films, 2003, 427, 137-141.	0.8	20
232	Property control of expanding thermal plasma deposited textured zinc oxide with focus on thin film solar cell applications. Thin Solid Films, 2005, 492, 298-306.	0.8	20
233	Interaction of SiH3 radicals with deuterated (hydrogenated) amorphous silicon surfaces. Surface Science, 2005, 598, 35-44.	0.8	20
234	Probing hydrogenated amorphous silicon surface states by spectroscopic and real-time second-harmonic generation. Physical Review B, 2006, 73, .	1.1	20

#	Article	IF	CITATIONS
235	Optical and chemical characterization of expanding thermal plasma-deposited carbon-containing silicon dioxide-like films. Thin Solid Films, 2008, 516, 8547-8553.	0.8	20
236	Cas-Phase Hydrosilylation of Plasma-Synthesized Silicon Nanocrystals with Short- and Long-Chain Alkynes. Langmuir, 2012, 28, 17295-17301.	1.6	20
237	Spontaneous synthesis of carbon nanowalls, nanotubes and nanotips using high flux density plasmas. Carbon, 2014, 68, 695-707.	5.4	20
238	Atmospheric-pressure diffuse dielectric barrier discharges in Ar/O ₂ gas mixture using 200 kHz/13.56 MHz dual frequency excitation. Journal Physics D: Applied Physics, 2018, 51, 114002.	1.3	20
239	Vibrational Kinetics in Plasma as a Functional Problem: A Flux-Matching Approach. Journal of Physical Chemistry A, 2018, 122, 7918-7923.	1.1	20
240	Application of a hybrid collisional radiative model to recombining argon plasmas. Journal of Quantitative Spectroscopy and Radiative Transfer, 1993, 49, 129-139.	1.1	19
241	Fabry–Pérot line shape analysis on an expanding cascaded arc plasma in argon. Journal of Applied Physics, 1994, 75, 2775-2780.	1.1	19
242	Plasma processing and chemistry. Plasma Physics and Controlled Fusion, 1994, 36, B65-B78.	0.9	19
243	Absolute in situ measurement of surface dangling bonds during a-Si:H growth. Applied Physics Letters, 2007, 90, 161918.	1.5	19
244	a-Si:Hâ^•c-Si heterointerface formation and epitaxial growth studied by real time optical probes. Applied Physics Letters, 2007, 90, 202108.	1.5	19
245	Reaction mechanisms and thin a-C:H film growth from low energy hydrocarbon radicals. Journal of Physics: Conference Series, 2007, 86, 012020.	0.3	19
246	Formation and Expansion Phases of an Atmospheric Pressure Glow Discharge in a PECVD Reactor via Fast ICCD Imaging. IEEE Transactions on Plasma Science, 2008, 36, 968-969.	0.6	19
247	Plasmaâ€enhanced Chemical Vapor Deposition of Aluminum Oxide Using Ultrashort Precursor Injection Pulses. Plasma Processes and Polymers, 2012, 9, 761-771.	1.6	19
248	Direct ion flux measurements at high-pressure-depletion conditions for microcrystalline silicon deposition. Journal of Applied Physics, 2013, 114, 063305.	1.1	19
249	Atomic layer deposition of cobalt phosphate thin films for the oxygen evolution reaction. Electrochemistry Communications, 2019, 98, 73-77.	2.3	19
250	Mode resolved heating dynamics in pulsed microwave CO2 plasma from laser Raman scattering. Journal Physics D: Applied Physics, 2020, 53, 054002.	1.3	19
251	Redefining the Microwave Plasma-Mediated CO ₂ Reduction Efficiency Limit: The Role of O–CO ₂ Association. ACS Energy Letters, 2021, 6, 2876-2881.	8.8	19
252	Plasma Driven Exsolution for Nanoscale Functionalization of Perovskite Oxides. Small Methods, 2021, 5, e2100868.	4.6	19

#	Article	IF	CITATIONS
253	Heterogeneous and homogeneous hydrogen kinetics in plasma chemistry. Plasma Sources Science and Technology, 1995, 4, 293-301.	1.3	18
254	Deposition of amorphous carbon layers from C2H2 and CF4 with an expanding thermal arc plasma beam set-up. Thin Solid Films, 1995, 271, 56-63.	0.8	18
255	Absence of the enhanced intra-4f transition cross section at 1.5μm of Er3+ in Si-rich SiO2. Applied Physics Letters, 2005, 86, 241109.	1.5	18
256	ALD Options for Si-integrated Ultrahigh-density Decoupling Capacitors in Pore and Trench Designs. ECS Transactions, 2007, 3, 173-181.	0.3	18
257	Probing the phase composition of silicon films in situ by etch product detection. Applied Physics Letters, 2007, 91, 161902.	1.5	18
258	A hard graphitelike hydrogenated amorphous carbon grown at high deposition rate (>15nmâ^•s). Applied Physics Letters, 2008, 92, 221502.	1.5	18
259	Silicon surface passivation by hot-wire CVD Si thin films studied by in situ surface spectroscopy. Thin Solid Films, 2009, 517, 3456-3460.	0.8	18
260	Synergistic etch rates during low-energetic plasma etching of hydrogenated amorphous carbon. Journal of Applied Physics, 2012, 112, .	1.1	18
261	Gas temperature in transient CO2plasma measured by Raman scattering. Journal Physics D: Applied Physics, 2015, 48, 155201.	1.3	18
262	Synergy Between Plasmaâ€Assisted ALD and Rollâ€ŧoâ€Roll Atmospheric Pressure PE VD Processing of Moisture Barrier Films on Polymers. Plasma Processes and Polymers, 2016, 13, 311-315.	1.6	18
263	Preferential vibrational excitation in microwave nitrogen plasma assessed by Raman scattering. Plasma Sources Science and Technology, 2018, 27, 055006.	1.3	18
264	Evidence for charge exchange between N+ and N2(A3Σ+u) in a low-temperature nitrogen plasma. Chemical Physics Letters, 1998, 290, 379-384.	1.2	17
265	A model for the deposition of a-C:H using an expanding thermal arc. Surface and Coatings Technology, 1998, 98, 1584-1589.	2.2	17
266	Surface roughness evolution of a-Si:H growth and its relation to the growth mechanism. Materials Research Society Symposia Proceedings, 2000, 609, 761.	0.1	17
267	In Situ Probing and Atomistic Simulation of a-Si:H Plasma Deposition. Materials Research Society Symposia Proceedings, 2001, 664, 111.	0.1	17
268	Carbon monoxide-induced reduction and healing of graphene oxide. Journal of Vacuum Science and Technology A: Vacuum, Surfaces and Films, 2013, 31, .	0.9	17
269	Dielectric barrier discharges revisited: the case for mobile surface charge. Plasma Sources Science and Technology, 2016, 25, 03LT03.	1.3	17
270	Atomic layer deposition of highly dispersed Pt nanoparticles on a high surface area electrode backbone for electrochemical promotion of catalysis. Electrochemistry Communications, 2017, 84, 40-44.	2.3	17

#	Article	IF	CITATIONS
271	Solar Hydrogen Generation from Ambient Humidity Using Functionalized Porous Photoanodes. ACS Applied Materials & Interfaces, 2019, 11, 41267-41280.	4.0	17
272	Ion densities in a high-intensity, low flow nitrogen–argon plasma. Physics of Plasmas, 1997, 4, 3077-3081.	0.7	16
273	Remote Silane Plasma Chemistry Effects and their Correlation with a-Si:H Film Properties. Materials Research Society Symposia Proceedings, 1999, 557, 25.	0.1	16
274	High rate (â^¼3 nm/s) deposition of dense silicon nitride films at low substrate temperatures (<150 °C) using the expanding thermal plasma and substrate biasing. Thin Solid Films, 2005, 484, 46-53.	0.8	16
275	SiHx film growth precursors during high-rate nanocrystalline silicon deposition. Journal of Applied Physics, 2006, 99, 076110.	1.1	16
276	Improved adhesion and tribological properties of fast-deposited hard graphite-like hydrogenated amorphous carbon films. Diamond and Related Materials, 2011, 20, 1266-1272.	1.8	16
277	Gasâ€Phase Plasma Synthesis of Freeâ€Standing Silicon Nanoparticles for Future Energy Applications. Plasma Processes and Polymers, 2016, 13, 19-53.	1.6	16
278	Plasma and surface chemistry effects during high rate deposition of hydrogenated amorphous silicon. Plasma Physics and Controlled Fusion, 1999, 41, A365-A378.	0.9	15
279	In situ single wavelength ellipsometry studies of high rate hydrogenated amorphous silicon growth using a remote expanding thermal plasma. Journal of Applied Physics, 2000, 88, 6388-6394.	1.1	15
280	Substrate temperature dependence of the roughness evolution of HWCVD a-Si:H studied by real-time spectroscopic ellipsometry. Thin Solid Films, 2006, 501, 88-91.	0.8	15
281	Views on Macroscopic Kinetics of Plasma Polymerization: Acrylic Acid Revisited. Plasma Processes and Polymers, 2010, 7, 887-888.	1.6	15
282	Hydrogenated amorphous silicon deposited under accurately controlled ion bombardment using pulse-shaped substrate biasing. Journal of Applied Physics, 2010, 108, 103304.	1.1	15
283	Microfocus infrared ellipsometry characterization of air-exposed graphene flakes. Applied Physics Letters, 2011, 99, 061909.	1.5	15
284	Surface Dynamics of SiO ₂ â€like Films on Polymers Grown by DBD Assisted CVD at Atmospheric Pressure. Plasma Processes and Polymers, 2012, 9, 1194-1207.	1.6	15
285	The electrochemistry of iron oxide thin films nanostructured by high ion flux plasma exposure. Electrochimica Acta, 2017, 258, 709-717.	2.6	15
286	Amorphous silicon layer characteristics during 70–2000eV Ar+-ion bombardment of Si(100). Journal of Vacuum Science and Technology A: Vacuum, Surfaces and Films, 2006, 24, 1933-1940.	0.9	14
287	Downstream ion and radical densities in an Ar–NH3plasma generated by the expanding thermal plasma technique. Plasma Sources Science and Technology, 2006, 15, 546-555.	1.3	14
288	Hybrid Sputteringâ€Remote PECVD Deposition of Au Nanoparticles on SiO ₂ Layers for Surface Plasmon Resonanceâ€Based Colored Coatings. Plasma Processes and Polymers, 2010, 7, 657-664.	1.6	14

#	Article	IF	CITATIONS
289	Plasma-Assisted Deposition of Au/SiO2 Multi-layers as Surface Plasmon Resonance-Based Red-Colored Coatings. Plasmonics, 2011, 6, 255-260.	1.8	14
290	Influence of molecular processes on the hydrogen atomic system in an expanding argon–hydrogen plasma. Physics of Plasmas, 1995, 2, 1002-1008.	0.7	13
291	Hydrogen Incorporation During Deposition of a-Si:H From an Intense Source of SiH ₃ . Materials Research Society Symposia Proceedings, 1997, 467, 621.	0.1	13
292	Optical Characterization of Plasmaâ€Deposited SiO ₂ â€Like Layers on Anisotropic Polymeric Substrates. Plasma Processes and Polymers, 2010, 7, 766-774.	1.6	13
293	Morphological Description of Ultra‣mooth Organo‣ilicone Layers Synthesized Using Atmospheric Pressure Dielectric Barrier Discharge Assisted PECVD. Plasma Processes and Polymers, 2013, 10, 313-319.	1.6	13
294	The impact of the nano-pore filling on the performance of organosilicon-based moisture barriers. Thin Solid Films, 2015, 595, 251-257.	0.8	13
295	Special Issue of Papers by Plenary and Topical Invited Lecturers at the 22nd International Symposium on Plasma Chemistry (ISPC 22), 5–10 July 2015, Antwerp, Belgium: Introduction. Plasma Chemistry and Plasma Processing, 2016, 36, 1-2.	1.1	13
296	Enhancing the Electrocatalytic Activity of Redox Stable Perovskite Fuel Electrodes in Solid Oxide Cells by Atomic Layer-Deposited Pt Nanoparticles. ACS Sustainable Chemistry and Engineering, 2020, 8, 12646-12654.	3.2	13
297	Experimental characterization of a hydrogen/argon cascaded arc plasma source. Review of Scientific Instruments, 1994, 65, 1469-1471.	0.6	12
298	On the Effect of Substrate Temperature on a-Si:H Deposition Using an Expanding Thermal Plasma. Materials Research Society Symposia Proceedings, 1996, 420, 341.	0.1	12
299	High-rate deposition of microcrystalline silicon with an expanding thermal plasma. Thin Solid Films, 2005, 491, 280-293.	0.8	12
300	Hidden parameters in the plasma deposition of microcrystalline silicon solar cells. Journal of Materials Research, 2007, 22, 1767-1774.	1.2	12
301	Role of a‣i:H bulk in surface passivation of c‣i wafers. Physica Status Solidi - Rapid Research Letters, 2010, 4, 172-174.	1.2	12
302	The role of the gradient film properties in silica moisture barriers synthesized in a rollâ€toâ€roll atmospheric pressure plasma enhanced CVD reactor. Plasma Processes and Polymers, 2018, 15, 1700093.	1.6	12
303	Numerical simulation of atmospheric-pressure 200 kHz/13.56 MHz dual-frequency dielectric barrier discharges. Plasma Sources Science and Technology, 2018, 27, 105016.	1.3	12
304	Plasma radiation studies in Magnum-PSI using resistive bolometry. Nuclear Fusion, 2018, 58, 106006.	1.6	12
305	Emission spectroscopy of He lines in high-density plasmas in Magnum-PSI. AIP Advances, 2020, 10, .	0.6	12
306	Operando attenuated total reflection Fourier-transform infrared (ATR-FTIR) spectroscopy for water splitting. Journal Physics D: Applied Physics, 2021, 54, 133001.	1.3	12

#	Article	IF	CITATIONS
307	Fast deposition of amorphous carbon and silicon layers. Journal of Nuclear Materials, 1993, 200, 430-433.	1.3	11
308	Investigation of processes in low-pressure expanding thermal plasmas used for carbon nitride deposition: II. Ar/N2plasma with graphite nozzle. Plasma Sources Science and Technology, 2001, 10, 524-529.	1.3	11
309	Initial growth and properties of atomic layer deposited TiN films studied byin situ spectroscopic ellipsometry. Physica Status Solidi C: Current Topics in Solid State Physics, 2005, 2, 3958-3962.	0.8	11
310	Nitrogen incorporation during metal organic chemical vapor deposition of ZnO films using a remote Arâ^•N2 plasma. Applied Physics Letters, 2006, 89, 022110.	1.5	11
311	Spectroscopic second-harmonic generation duringAr+-ion bombardment of Si(100). Physical Review B, 2006, 74, .	1.1	11
312	Attenuated total reflection infrared spectroscopy for studying adsorbates on planar model catalysts: CO adsorption on silica supported Rh nanoparticles. Journal of Vacuum Science and Technology A: Vacuum, Surfaces and Films, 2006, 24, 296-304.	0.9	11
313	Real time spectroscopic ellipsometry on ultrathin (<50Ã) hydrogenated amorphous silicon films on Si(100) and GaAs(100). Journal of Applied Physics, 2007, 101, 123529.	1.1	11
314	(Invited) All-Solid-State Batteries: A Challenging Route towards 3D Integration. ECS Transactions, 2010, 33, 213-222.	0.3	11
315	Shape Memory Polymer Thin Films Deposited by Initiated Chemical Vapor Deposition. Macromolecules, 2010, 43, 8344-8347.	2.2	11
316	Analysis of temporal evolution of quantum dot surface chemistry by surface-enhanced Raman scattering. Scientific Reports, 2016, 6, 29508.	1.6	11
317	Nanostructuring of iron thin films by high flux low energy helium plasma. Thin Solid Films, 2017, 631, 50-56.	0.8	11
318	Charged particle kinetics and gas heating in CO ₂ microwave plasma contraction: comparisons of simulations and experiments. Plasma Sources Science and Technology, 2022, 31, 055005.	1.3	11
319	Supersonically expanding cascaded arc plasma properties: comparison of Ne, Ar and Xe. Plasma Sources Science and Technology, 2003, 12, 107-118.	1.3	10
320	A capacitive probe with shaped probe bias for ion flux measurements in depositing plasmas. Review of Scientific Instruments, 2008, 79, 115104.	0.6	10
321	Hydrogenated amorphous silicon based surface passivation of c‣i at high deposition temperature and rate. Physica Status Solidi - Rapid Research Letters, 2010, 4, 206-208.	1.2	10
322	Remote plasma deposition of microcrystalline silicon thin-films: Film structure and the role of atomic hydrogen. Journal of Non-Crystalline Solids, 2012, 358, 379-386.	1.5	10
323	Chemical sputtering of graphite by low temperature nitrogen plasmas at various substrate temperatures and ion flux densities. Journal of Applied Physics, 2013, 114, .	1.1	10
324	Nucleation of silicon nanocrystals in a remote plasma without subsequent coagulation. Journal of Applied Physics, 2014, 115, 244301.	1.1	10

#	Article	IF	CITATIONS
325	Mechanisms of elementary hydrogen ion-surface interactions during multilayer graphene etching at high surface temperature as a function of flux. Carbon, 2018, 137, 527-532.	5.4	10
326	High-Throughput Computational Screening of Cubic Perovskites for Solid Oxide Fuel Cell Cathodes. Journal of Physical Chemistry Letters, 2021, 12, 4160-4165.	2.1	10
327	Rational Design of Photoelectrodes for the Fully Integrated Polymer Electrode Membrane–Photoelectrochemical Water-Splitting System: A Case Study of Bismuth Vanadate. ACS Applied Energy Materials, 2021, 4, 9600-9610.	2.5	10
328	How the alternating degeneracy in rotational Raman spectra of CO2and C2H2reveals the vibrational temperature. Applied Optics, 2018, 57, 5694.	0.9	10
329	The Chemical Origins of Plasma Contraction and Thermalization in CO ₂ Microwave Discharges. Journal of Physical Chemistry Letters, 2022, 13, 1203-1208.	2.1	10
330	On expanding recombining plasma for fast deposition of a-Si:H thin films. Plasma Sources Science and Technology, 1994, 3, 521-527.	1.3	9
331	The Role of H in the Growth Mechanism of PECVD a-Si:H. Materials Research Society Symposia Proceedings, 1999, 557, 13.	0.1	9
332	High-rate deposition of nanocrystalline silicon using the expanding thermal plasma technique. Journal of Non-Crystalline Solids, 2006, 352, 915-918.	1.5	9
333	High-Rate Anisotropic Silicon Etching with the Expanding Thermal Plasma Technique. Electrochemical and Solid-State Letters, 2007, 10, H309.	2.2	9
334	Population inversion in a magnetized hydrogen plasma expansion as a consequence of the molecular mutual neutralization process. Physical Review E, 2011, 83, 036412.	0.8	9
335	Improved conductivity of aluminum-doped ZnO: The effect of hydrogen diffusion from a hydrogenated amorphous silicon capping layer. Journal of Applied Physics, 2012, 111, 063715.	1.1	9
336	Controlling the resistivity gradient in aluminum-doped zinc oxide grown by plasma-enhanced chemical vapor deposition. Journal of Applied Physics, 2012, 112, .	1.1	9
337	In situ crystallization kinetics studies of plasma-deposited, hydrogenated amorphous silicon layers. Journal of Applied Physics, 2012, 111, 033508.	1.1	9
338	High throughput deposition of hydrogenated amorphous carbon coatings on rubber with expanding thermal plasma. Surface and Coatings Technology, 2014, 245, 74-83.	2.2	9
339	Relation between light trapping and surface topography of plasma textured crystalline silicon wafers. Progress in Photovoltaics: Research and Applications, 2015, 23, 352-366.	4.4	9
340	Improving uniformity of atmospheric-pressure dielectric barrier discharges using dual frequency excitation. Plasma Sources Science and Technology, 2018, 27, 01LT01.	1.3	9
341	An Expanding Thermal Plasma for Deposition of a-Si:H. Materials Research Society Symposia Proceedings, 1995, 377, 33.	0.1	8
342	Langmuir probe measurements in expanding magnetized argon, nitrogen and hydrogen plasmas. Surface and Coatings Technology, 1998, 98, 1416-1419.	2.2	8

#	Article	IF	CITATIONS
343	The expanding thermal arc plasma: the low-flow regime. Plasma Sources Science and Technology, 1998, 7, 28-35.	1.3	8
344	The role of the silyl radical in plasma deposition of microcrystalline silicon. Journal of Applied Physics, 2004, 96, 4076-4083.	1.1	8
345	Expanding thermal plasma-deposited ZnO films: Substrate temperature influence on films properties. Film growth studies. Superlattices and Microstructures, 2006, 39, 348-357.	1.4	8
346	Plasma-Enhanced ALD of TiO ₂ Using a Novel Cyclopentadienyl Alkylamido Precursor [Ti(Cp ^{Me})(NMe ₂) ₃] and O ₂ Plasma. ECS Transactions, 2010, 33, 385-393.	0.3	8
347	Amorphization of Si(100) by Ar+-ion bombardment studied with spectroscopic and time-resolved second-harmonic generation. Journal of Vacuum Science and Technology A: Vacuum, Surfaces and Films, 2010, 28, 293-301.	0.9	8
348	Solid-phase crystallization of ultra high growth rate amorphous silicon films. Journal of Applied Physics, 2012, 111, 103510.	1.1	8
349	An improved thin film approximation to accurately determine the optical conductivity of graphene from infrared transmittance. Applied Physics Letters, 2014, 105, 013105.	1.5	8
350	The role of carrier gas flow in roll-to-roll AP-PECVD synthesized silica moisture barrier films. Surface and Coatings Technology, 2018, 339, 20-26.	2.2	8
351	Revisiting spontaneous Raman scattering for direct oxygen atom quantification. Optics Letters, 2021, 46, 2172.	1.7	8
352	Resolving discharge parameters from atomic oxygen emission. Plasma Sources Science and Technology, 2021, 30, 065022.	1.3	8
353	Quantum Magnetoconductance of the Two-Dimensional Electron Gas on a Liquid Helium Surface. Japanese Journal of Applied Physics, 1987, 26, 749.	0.8	8
354	Generalized law of mass action for a two-temperature plasma. Physical Review A, 1991, 44, 5150-5157.	1.0	7
355	Vibrational Population of Hydrogen Molecules Excited by an RF Discharge in an Expanding Thermal Arc Plasma as Determined by Emission Spectroscopy. Contributions To Plasma Physics, 1995, 35, 195-202.	0.5	7
356	An approximate quantitative analysis of non-equilibrium plasma transport for high density plasmas. Plasma Chemistry and Plasma Processing, 1995, 16, S19-S42.	1.1	7
357	Material properties and growth process of microcrystalline silicon with growth rates in excess of 1 nm/s. Materials Research Society Symposia Proceedings, 2001, 664, 421.	0.1	7
358	Expanding Thermal Plasma Deposition of Silicon Dioxide-Like Films for Microelectronic Devices. Materials Research Society Symposia Proceedings, 2002, 715, 1931.	0.1	7
359	Optoelectronic properties of expanding thermal plasma deposited textured zinc oxide: Effect of aluminum doping. Journal of Electronic Materials, 2006, 35, 711-716.	1.0	7
360	Remote Plasma-Enhanced Metalorganic Chemical Vapor Deposition of Aluminum Oxide Thin Films. Plasma Processes and Polymers, 2008, 5, 645-652.	1.6	7

#	Article	IF	CITATIONS
361	Hot-wire deposition of a-Si:H thin films on wafer substrates studied by real-time spectroscopic ellipsometry and infrared spectroscopy. Thin Solid Films, 2008, 516, 511-516.	0.8	7
362	Comparison between aluminum oxide surface passivation films deposited with thermal ALD, plasma ALD and PECVD. , 2010, , .		7
363	Ion probe detection of clusters in a remotely expanding thermal plasma. Plasma Sources Science and Technology, 2010, 19, 065012.	1.3	7
364	Defect prevention in silica thin films synthesized using AP-PECVD for flexible electronic encapsulation. Journal Physics D: Applied Physics, 2017, 50, 25LT01.	1.3	7
365	Electrochemistry of Sputtered Hematite Photoanodes: A Comparison of Metallic DC versus Reactive RF Sputtering. ACS Omega, 2019, 4, 9262-9270.	1.6	7
366	Operational Strategies to Improve the Performance and Longâ€Term Cyclability of Intermediate Temperature Sodiumâ€Sulfur Batteries. ChemElectroChem, 2021, 8, 1156-1166.	1.7	7
367	Absolute density of the argon first excited states in plasmas used for carbon deposition as determined by absorption spectroscopy. Diamond and Related Materials, 1995, 4, 1271-1276.	1.8	6
368	External rf substrate biasing during a-Si:H film growth using the expanding thermal plasma technique. Materials Research Society Symposia Proceedings, 2004, 808, 479.	0.1	6
369	Vapor Pressures of Precursors for the Chemical Vapor Deposition of Silicon-Based Films. Chemical Vapor Deposition, 2004, 10, 20-22.	1.4	6
370	Plasma Processes and Film Growth of Expanding Thermal Plasma Deposited Textured Zinc Oxide. Plasma Processes and Polymers, 2005, 2, 618-626.	1.6	6
371	Influence of rarefaction on the flow dynamics of a stationary supersonic hot-gas expansion. Physical Review E, 2008, 77, 036703.	0.8	6
372	On the surface roughness development of hydrogenated amorphous silicon deposited at low growth rates. Applied Physics Letters, 2009, 95, 021503.	1.5	6
373	Detailed H(<i>n</i> = 2) density measurements in a magnetized hydrogen plasma jet. Plasma Sources Science and Technology, 2012, 21, 024009.	1.3	6
374	Atomistic simulations of graphite etching at realistic time scales. Chemical Science, 2017, 8, 7160-7168.	3.7	6
375	Atmospheric-pressure silica-like thin film deposition using 200 kHz/13.56 MHz dual frequency excitation. Journal Physics D: Applied Physics, 2019, 52, 355201.	1.3	6
376	Charge carrier dynamics and photocatalytic activity of {111} and {100} faceted Ag3PO4 particles. Journal of Chemical Physics, 2020, 152, 244710.	1.2	6
377	A new absorption spectroscopy setup for the sensitive monitoring of atomic and molecular densities. Review of Scientific Instruments, 1995, 66, 968-974.	0.6	5
378	Plasma-surface interaction and surface diffusion during silicon-based thin-film growth. IEEE Transactions on Plasma Science, 2005, 33, 234-235.	0.6	5

#	Article	IF	CITATIONS
379	On the H-exchange of ammonia and silica hydroxyls in the presence of Rh nanoparticles. Applied Surface Science, 2007, 253, 3600-3607.	3.1	5
380	Ion-radical synergy in HfO2 etching studied with a XeF2/Ar+ beam setup. Journal of Applied Physics, 2008, 103, 083304.	1.1	5
381	Corona charging and optical second-harmonic generation studies of the field-effect passivation of c-SI by Al <inf>2</inf> 0 <inf>3</inf> films. , 2010, , .		5
382	Ion-induced effects on grain boundaries and <i>a</i> -Si:H tissue quality in microcrystalline silicon films. Journal of Vacuum Science and Technology A: Vacuum, Surfaces and Films, 2012, 30, .	0.9	5
383	Hydrogenated amorphous silicon p–i–n solar cells deposited under well controlled ion bombardment using pulseâ€shaped substrate biasing. Progress in Photovoltaics: Research and Applications, 2012, 20, 333-342.	4.4	5
384	Kinetic study of solid phase crystallisation of expanding thermal plasma deposited a-Si:H. Thin Solid Films, 2012, 520, 5820-5825.	0.8	5
385	Expanding Thermal Plasma Deposition of Alâ€Doped ZnO: On the Effect of the Plasma Chemistry on Film Growth Mechanisms. Plasma Processes and Polymers, 2016, 13, 54-69.	1.6	5
386	Fast nanostructured carbon microparticle synthesis by one-step high-flux plasma processing. Carbon, 2017, 124, 403-414.	5.4	5
387	Atomic hydrogen induced defect kinetics in amorphous silicon. Journal of Vacuum Science and Technology A: Vacuum, Surfaces and Films, 2017, 35, 05C307.	0.9	5
388	Infrared gas phase study on plasma-polymer interactions in high-current diffuse dielectric barrier discharge. Journal of Applied Physics, 2017, 121, 243301.	1.1	5
389	28. Plasma-based CO ₂ conversion. , 2019, , 585-634.		5
390	Novel Amorphous Silicon Solar Cell using a Manufacturing Procedure with a Temporary Superstrate. Materials Research Society Symposia Proceedings, 1999, 557, 713.	0.1	4
391	Ex situ and in situ defect density measurements of a-Si:H by means of the cavity ring down absorption technique. Materials Research Society Symposia Proceedings, 2001, 664, 2241.	0.1	4
392	High-rate deposition of a-SiN <i>_x</i> :H films for photovoltaic applications. Materials Research Society Symposia Proceedings, 2001, 664, 861.	0.1	4
393	New ultrahigh vacuum setup and advanced diagnostic techniques for studying a-Si:H film growth by radical beams. Materials Research Society Symposia Proceedings, 2004, 808, 491.	0.1	4
394	Plasma-assisted Atomic Layer Deposition of TiN Films at low Deposition Temperature for High-aspect Ratio Applications. Materials Research Society Symposia Proceedings, 2005, 863, B6.4-1.	0.1	4
395	Characterization of Nanocrystal Size Distribution using Raman Spectroscopy with a Multi-particle Phonon Confinement Model. Journal of Visualized Experiments, 2015, , e53026.	0.2	4
396	Residual gas entering high density hydrogen plasma: rarefaction due to rapid heating. Plasma Sources Science and Technology, 2015, 24, 025020.	1.3	4

#	Article	IF	CITATIONS
397	Non-equilibrium Microwave Plasma for Efficient High Temperature Chemistry. Journal of Visualized Experiments, 2017, , .	0.2	4
398	Variable roughness development in statically deposited SiO ₂ thin films: a spatially resolved surface morphology analysis. Journal Physics D: Applied Physics, 2018, 51, 285303.	1.3	4
399	Role of Electron–lon Dissociative Recombination in \$\$hbox {CH}_{4}\$\$ Microwave Plasma on Basis of Simulations and Measurements of Electron Energy. Plasma Chemistry and Plasma Processing, 2019, 39, 1275-1289.	1.1	4
400	Absorption and stimulated emission between the electronic states of C and C2radicals in an expanding thermal plasma. Plasma Sources Science and Technology, 1995, 4, 142-146.	1.3	3
401	Atomic hydrogen and argon ground state density determination in a recombining plasma using visible light absorption spectroscopy. Journal Physics D: Applied Physics, 1995, 28, 1362-1368.	1.3	3
402	Fundamentals and application of an expanding hydrogen low-pressure plasma jet. Vacuum, 1996, 47, 1123-1127.	1.6	3
403	Molecular Activated Recombination in Detached Recombining Plasmas. Physical Review Letters, 1999, 82, 2215-2215.	2.9	3
404	Relation between Growth Precursors and Film Properties for Plasma Deposition of a-Si:H at Rates up to 100 Ã/s. Materials Research Society Symposia Proceedings, 2000, 609, 421.	0.1	3
405	Modeling of the formation of cationic silicon clusters in a remote Ar/H2/SiH4 plasma. Journal of Applied Physics, 2000, 88, 537-543.	1.1	3
406	Integration of Expanding Thermal Plasma deposited Hydrogenated Amorphous Silicon in Solar Cells. Materials Research Society Symposia Proceedings, 2002, 715, 651.	0.1	3
407	The a-Si:H Growth Mechanism: Temperature Study of the SiH3 Surface Reactivity and the Surface Silicon Hydride Composition During Film Growth. Materials Research Society Symposia Proceedings, 2003, 762, 931.	0.1	3
408	Two-photon absorption laser induced fluorescence on O and O3 in a dc plasma for oxidation of aluminum. Journal of Vacuum Science and Technology A: Vacuum, Surfaces and Films, 2004, 22, L11-L14.	0.9	3
409	New insights in microcrystalline silicon deposition with expanding thermal plasma chemical vapor deposition. Journal of Non-Crystalline Solids, 2006, 352, 933-936.	1.5	3
410	Remote Plasma and Thermal ALD of Al2O3 for Trench Capacitor Applications. ECS Transactions, 2007, 3, 67-77.	0.3	3
411	Densification of thin a-C : H films grown from low-kinetic energy hydrocarbon radicals under the influence of H and C particle fluxes: a molecular dynamics study. Journal Physics D: Applied Physics, 2006, 39, 1948-1953.	1.3	3
412	H ₂ : The Critical Juncture between Polymerization and Dissociation of Hydrocarbons in a Lowâ€ŧemperature Plasma. Plasma Processes and Polymers, 2011, 8, 832-841.	1.6	3
413	Improved size distribution control of silicon nanocrystals in a spatially confined remote plasma. Plasma Sources Science and Technology, 2015, 24, 015030.	1.3	3
414	Control of the intrinsic microstructure in AP-PECVD synthesised amorphous silica thin films. RSC Advances, 2017, 7, 52274-52282.	1.7	3

#	Article	IF	CITATIONS
415	An analytical force balance model for dust particles with size up to several Debye lengths. Physics of Plasmas, 2017, 24, 113702.	0.7	3
416	Fokker–Planck equation for chemical reactions in plasmas. Rendiconti Lincei, 2019, 30, 25-30.	1.0	3
417	Flame bands: CO + O chemiluminescence as a measure of gas temperature. Journal Physics D: Applied Physics, 2021, 54, 374005.	1.3	3
418	Reply to â€~â€~Saha equation for a two-temperature plasma''. Physical Review A, 1990, 42, 2461-2462.	1.0	2
419	The diagnostics of thermal plasmas. Pure and Applied Chemistry, 1992, 64, 645-652.	0.9	2
420	Absorption spectroscopy measurements of atomic and molecular carbon population densities in an expanding thermal arc plasma. Diamond and Related Materials, 1995, 4, 908-911.	1.8	2
421	Hard Amorphous Hydrogenated Carbon Films Deposited from an Expanding Thermal Plasma. Materials Research Society Symposia Proceedings, 1996, 436, 287.	0.1	2
422	Fast deposition of thin amorphous layers using an expanding thermal plasma. Pure and Applied Chemistry, 1996, 68, 1155-1158.	0.9	2
423	Importance of Defect Density near the p-i Interface for a-Si:H Solar Cell Performance. Materials Research Society Symposia Proceedings, 2001, 664, 2441.	0.1	2
424	Wall-association processes in expanding thermal hydrogen plasmas. IEEE Transactions on Plasma Science, 2002, 30, 146-147.	0.6	2
425	Design of a fastin situinfrared diagnostic tool. Review of Scientific Instruments, 2003, 74, 2675-2684.	0.6	2
426	Roughness evolution of high-rate deposited a-SiNx:H films studied by atomic force microscopy and real time spectroscopic ellipsometry. Materials Research Society Symposia Proceedings, 2004, 808, 532.	0.1	2
427	Electron beam induced fluorescence measurements of the degree of hydrogen dissociation in hydrogen plasmas. Plasma Sources Science and Technology, 2004, 13, 729-738.	1.3	2
428	Spectroscopic second harmonic generation as a diagnostic tool in silicon materials processing. Physica Status Solidi C: Current Topics in Solid State Physics, 2005, 2, 3968-3972.	0.8	2
429	Influence of hydrogen dilution on surface roughness development of a-Si:H thin films grown by remote plasma deposition. Physica Status Solidi C: Current Topics in Solid State Physics, 2010, 7, NA-NA.	0.8	2
430	On the effect of the underlying ZnO:Al layer on the crystallization kinetics of hydrogenated amorphous silicon. Applied Physics Letters, 2013, 102, .	1.5	2
431	On the synergistic effect of inorganic/inorganic barrier layers: An ellipsometric porosimetry investigation. Plasma Processes and Polymers, 2017, 14, 1700012.	1.6	2
432	The Saha Equation for a Two-Temperature Plasma. Teubner-Texte Zur Physik, 1992, , 81-86.	3.0	2

#	Article	lF	CITATIONS
433	Material Structure of Microcrystalline Silicon Deposited with an Expanding Thermal Plasma. Materials Research Society Symposia Proceedings, 2003, 762, 1531.	0.1	2
434	Thin Film Cavity Ringdown Spectroscopy and Second Harmonic Generation on Thin a-Si:H Films. Materials Research Society Symposia Proceedings, 2003, 762, 1981.	0.1	2
435	Influence of the addition of CF4 on the deposition of a-C:H layers using the expanding thermal plasma technique. Diamond and Related Materials, 1995, 4, 328-332.	1.8	1
436	Textured Zinc Oxide by Expanding Thermal Plasma CVD: the Effect of Aluminum Doping. Materials Research Society Symposia Proceedings, 2002, 730, 1.	0.1	1
437	Gas phase deposition of hybrid coatings. Materials Research Society Symposia Proceedings, 2002, 726, 1.	0.1	1
438	Highly Efficient Microcrystalline Silicon Solar Cells Deposited from a Pure SiH4 Flow. Materials Research Society Symposia Proceedings, 2006, 910, 1.	0.1	1
439	High-Rate Anisotropic Silicon Etching with the Expanding Thermal Plasma Technique. ECS Transactions, 2006, 3, 291-298.	0.3	1
440	Optimisation of Microcrystaline Silicon Deposited by Expanding Thermal Plasma Chemical Vapor Deposition for Solar-Cell Application. Materials Research Society Symposia Proceedings, 2007, 989, 2.	0.1	1
441	Manipulating the Hydrogen-Bonding Configuration in ETP-CVD a-Si:H. Materials Research Society Symposia Proceedings, 2007, 989, 4.	0.1	1
442	Roughening during XeF2 etching of Si(100) through interface layers: H:Si(100) and a-Siâ^•Si(100). Journal of Vacuum Science and Technology A: Vacuum, Surfaces and Films, 2009, 27, 367-375.	0.9	1
443	Ion Assisted ETP-CVD a-Si:H at Well Defined Ion Energies. Materials Research Society Symposia Proceedings, 2009, 1153, 1.	0.1	1
444	Studies into the Growth Mechanism of a-Si:H Usingin situ Cavity Ring-Down Techniques. , 0, , 237-271.		1
445	The Influence of Ions and Photons during Plasma-Assisted ALD of Metal Oxides. ECS Transactions, 2010, 33, 61-67.	0.3	1
446	17th International Summer School on Vacuum, Electron, and Ion Technologies (VEIT 2011). Journal of Physics: Conference Series, 2012, 356, 011001.	0.3	1
447	Back Cover: Plasma Process. Polym. 1â^•2016. Plasma Processes and Polymers, 2016, 13, 202-202.	1.6	1
448	Plasma conductivity as a probe for ambient air admixture in an atmospheric pressure plasma jet. Plasma Chemistry and Plasma Processing, 2018, 38, 63-74.	1.1	1
449	Visible detection of performance controlling pinholes in silica encapsulation films. Journal Physics D: Applied Physics, 2018, 51, 43LT01.	1.3	1
450	On the Role of Surface Diffusion and Its Relation to the Hydrogen Incorporation During Hydrogenated Amorphous Silicon Growth. Materials Research Society Symposia Proceedings, 2003, 762, 1031.	0.1	1

#	Article	IF	CITATIONS
451	Expanding thermal plasma for low-k dielectrics deposition. Materials Research Society Symposia Proceedings, 2003, 766, 691.	0.1	1
452	On the Surface Roughness Evolution During a-Si:H Growth. Materials Research Society Symposia Proceedings, 2002, 715, 1511.	0.1	1
453	Electrodeless thin film conductance measurements using the Sommer–Tanner method. Review of Scientific Instruments, 1996, 67, 3624-3626.	0.6	Ο
454	High-rate a-Si:H and μc-Si:H Film Growth Studied by Advanced Plasma and in situ Film Diagnostics. Materials Research Society Symposia Proceedings, 2002, 715, 2561.	0.1	0
455	Hydrogen Injection in ETP Plasma Jet for Fast-Deposition of High-Quality a-Si:H. Materials Research Society Symposia Proceedings, 2004, 808, 609.	0.1	0
456	Real-time study of HWCVD a-Si:H film growth using optical second harmonic generation spectroscopy. Thin Solid Films, 2006, 501, 70-74.	0.8	0
457	Advanced Plasma Diagnostics for Thin-Film Deposition. , 0, , 117-136.		0
458	The Cascaded Arc: High Flows of Rovibrationally Excited H[sub 2] and its Impact on H[sup â^'] Ion Formation. , 2009, , .		0
459	Investigating the flow dynamics and chemistry of an expanding thermal plasma through CH(A–X) emission spectra. Journal Physics D: Applied Physics, 2011, 44, 355205.	1.3	0
460	On the role of atomic hydrogen during microcrystalline silicon thin-film deposition. , 2011, , .		0
461	In-situ X-ray diffraction analysis of the crystallisation of a-SI:H films deposited by the expanding thermal plasma technique. , 2011, , .		0
462	PPPS-2013: CO <inf>2</inf> conversion in non-thermal plasma processes. , 2013, , .		0
463	PPPS-2013: Infrared gas phase studies and scaling parameters in PE-CVD processes at atmospheric pressure using high-current dielectric barrier discharges. , 2013, , .		0
464	VEIT 2014. Journal of Physics: Conference Series, 2014, 514, 011001.	0.3	0
465	Post-transit Analysis of Transient Photocurrents from High-Deposition-Rate a-Si:H Samples. Materials Research Society Symposia Proceedings, 2003, 762, 1961.	0.1	Ο
466	High-rate (> 1nm/s) and low-temperature (< 400°C) deposition of silicon nitride using an N2/SiH4 and NH3/SiH4 expanding thermal plasma. Materials Research Society Symposia Proceedings, 2003, 762, 1861.	0.1	0
467	Simulations of Buffer Layers in a-Si:H Thin Film Solar Cells Deposited with an Expanding Thermal Plasma. Materials Research Society Symposia Proceedings, 2003, 762, 751.	0.1	0
468	Nano-scale Spectroscopy with Ultra-high-Q Monolithic Optical Resonators. , 2007, , .		0

#	Article	IF	CITATIONS
469	Optical Diagnostics for High Electron Density Plasmas. NATO ASI Series Series B: Physics, 1993, , 279-290.	0.2	Ο